Implications of CMIP6 projected drying trends for 21st century Amazonian drought risk

Luke A Parsons[1]

[1]University of Washington

November 26, 2022

Abstract

Recent exceptionally hot droughts in Amazonia have highlighted the potential role of global warming in driving elevated fire risk and forest dieback. The previous generation of global climate models projected that eastern Amazonia would receive less future rainfall while western Amazonia would receive more rainfall, but many of these models disagreed on the sign of future precipitation trends in the region. Here Coupled Modeling Intercomparison Project, Phase 6 (CMIP6) models are used to examine the shifting risk of eastern Amazonian droughts under climate change. This new generation of models shows better agreement that the entire Amazonian basin will receive less future rainfall, with particularly strong agreement that eastern Amazonia will dry in the 21 century. These models suggest that global warming may be increasing the likelihood of exceptionally hot drought in the region, and by mid-century with unabated global warming, recent particularly warm and severe droughts will become more common. However, Amazonia is a region with a relatively sparse instrumental record that makes it difficult to test the ability of model simulations to reproduce observed long-term rainfall trends, and climate models have traditionally struggled to reproduce satellite-era observed trends in the region. These shortcomings highlight the need to improve confidence in global climate models'; ability to simulate future drought, even if more CMIP6 models agree on the sign of future rainfall trends.

Implications of CMIP6 projected drying trends for 21st century Amazonian drought risk

L. A. Parsons [1]

[1]Department of Atmospheric Sciences, University of Washington, Seattle, WA

Corresponding author: Luke Parsons (lakp@uw.edu)

Key Points:

- Coupled Modeling Intercomparison Project, Phase 6 models show better agreement that the Amazon will receive less future rainfall
- These simulations indicate that if global warming continues unabated, recent particularly warm and severe droughts will become more common
- CMIP6 models that simulate more drying over Amazonia tend to simulate a more 'El Nino like' tropical Pacific

Abstract

Recent exceptionally hot droughts in Amazonia have highlighted the potential role of global warming in driving elevated fire risk and forest dieback. The previous generation of global climate models projected that eastern Amazonia would receive less future rainfall while western Amazonia would receive more rainfall, but many of these models disagreed on the sign of future precipitation trends in the region. Here Coupled Modeling Intercomparison Project, Phase 6 (CMIP6) models are used to examine the shifting risk of eastern Amazonian droughts under climate change. This new generation of models shows better agreement that the entire Amazonian basin will receive less future rainfall, with particularly strong agreement that eastern Amazonia will dry in the 21st century. These models suggest that global warming may be increasing the likelihood of exceptionally hot drought in the region, and by mid-century with unabated global warming, recent particularly warm and severe droughts will become more common. However, Amazonia is a region with a relatively sparse instrumental record that makes it difficult to test the ability of model simulations to reproduce observed long-term rainfall trends, and climate models have traditionally struggled to reproduce satellite-era observed trends in the region. These shortcomings highlight the need to improve confidence in global climate models' ability to simulate future drought, even if more CMIP6 models agree on the sign of future rainfall trends.

Plain Language Summary

Recent exceptionally hot droughts in Amazonia have highlighted the potential role of global warming in driving elevated fire risk and forest dieback. The previous generation of global climate models used in the Intergovernmental Panel on Climate Change Fifth Assessment Report (IPCC AR5) projected that eastern Amazonia would receive less future rainfall while western Amazonia would receive more rainfall. Here climate models used in the upcoming IPCC Sixth Assessment Report (IPCC AR6) are used to examine future rainfall and temperature changes over tropical South America. The new generation of CMIP6 models shows better agreement that the entire Amazonian basin will receive less future rainfall, with particularly strong agreement that eastern Amazonia will dry in the future if the planet continues to warm. These models suggest that global warming has already increased the likelihood of exceptionally hot drought in the region, and by mid-century under business-as-usual warming, recent particularly warm and severe droughts will become more common. However, climate models traditionally struggle to reproduce several key observed rainfall metrics in this region.

1 Introduction

The Amazonian rainforest is a biodiversity hotspot (Mittermeier et al., 1998) that provides important ecosystem services both locally and globally (Malhi et al., 2008; Lenton et al., 2008). Yet, the composition of the Amazonian rainforest is vulnerable to human land use as well as climate variability and global climate change (Nepstad et al., 1994; Malhi et al., 2009; Marengo et al., 2018). A combination of warming and rainfall deficits, driven by both climate variability and change, will likely cause future ecosystem stress, and thus potentially limit the ability of this region to continue to store carbon (Tian et al., 1998; Phillips et al., 2009). Decreased seasonal precipitation and warming are already contributing to drought and vegetation stress in this region (Marengo et al., 2018; Lewis et al., 2011; Dai et al., 2013; Jimenez-Munoz et al., 2016; Saatchi et al., 2013). Specifically, fires during droughts in tropical South America can clear tropical rainforest and grassland, leading to carbon emissions to the atmosphere (Aragao et al., 2018); recent work has shown that rainfall deficits can increase fire risk, leading to self-amplified forest loss and a possible deforestation tipping point (Brando et al., 2014; Zemp et al., 2017; Boers et al., 2017) .

Superimposed on future rainfall changes (Duffy et al., 2017), the region will also need to cope with multi-year droughts arising from natural background climate variability (Parsons et al., 2018). The paleoclimate records suggests that the Amazonian ecosystem was able to persist during moderate droughts in the pre-industrial climate (Bush et al., 2016), but it is uncertain if future climate change, combined with other anthropogenic stressors and natural hydroclimatic variability, will trigger unprecedented and rapid forest dieback in this 'climate change hotspot' (Davidson et al., 2012; Diffenbaugh and Giorgi, 2012). The region is expected to warm quickly as the globe warms (Soares et al., 2019), but action that will limit future global climate change may significantly reduce the most detrimental impacts of climate change locally (Lehner et al., 2017).

The previous generation of climate models (Coupled Model Intercomparison Project Phase 5, or CMIP5) indicated that northeastern Amazonia may dry while western Amazonia may receive increasing rainfall as the globe warms (Duffy et al., 2015). Recent work has shown that the new Coupled Model Intercomparison Project Phase 6 (CMIP6) simulations agree on the sign of decreasing future rainfall trends in Amazonia, with droughts projected to increase in duration and intensity with global warming (Ukkola et al., 2020). Specifically, CMIP6 models show drying across western Amazonia, and most CMIP6 models agree on future decreases in soil moisture and runoff across most of Amazonia in low, medium, and high greenhouse gas emissions scenarios (Cook et al., 2020).

Studies of observed rainfall and temperature indicate that climate change may already be driving 'enhanced drought' in the region; 2016 was the warmest year in Amazonia since 1950 CE (Marengo et al., 2018), and the recent 2015-2016 drought in eastern Amazonia was at least 1.5ºC warmer than the drought associated with the 1997-1998 El Niño event (Jimenez-Munoz et al., 2016; hereafter JM16). Yet, the risk of this type of recent 'enhanced hot' drought (JM16) has not been investigated in state-of-the-art climate models, and recent preliminary studies of future drought changes in CMIP6 (e.g., Cook et al., 2020; Ukkola, 2020) have relied on limited numbers of these new model simulations (e.g., 10-13 models). Given the severity of recent seasonal droughts in the region and the apparent increase in model agreement in terms of future drying in the region, here instrumental records and an expanded suite of CMIP6 climate and Earth system model simulations are used to examine recent and future trends in rainfall and temperatures, with a focus on the likelihood of the risk of a 2015-2016 type 'enhanced drought' event (JM16) under a shifting precipitation baseline.

2 Data and Methods

2.1 Choice of season and drought metric

Surface air temperature variability and rainfall variability and trends over tropical Central and South America in October-March (ONDJFM) is examined (e.g., Satyamurty et al., 2010; Wang et al., 2018), with a specific focus on northeastern Amazonia (10ºS-8º N, 60ºW-50º W, outlined in Figure 1). Although many CMIP6 models project drying across much of tropical

South America (Ukkola, 2020; Cook et al., 2020), this study focuses on northeastern Amazonia due to the impact of recent drought in this region in observations (JM16), as well as the robust drying response in CMIP6 models in this region under climate change (Cook et al., 2020, also discussed here). Furthermore, although abnormally low rainfall can occur during various months throughout the year, here the focus is on ONDJFM due to the impacts of El Niño events during the time period (e.g., JM16). Precipitation is chosen to study the impacts of climate change on drought because many other drought metrics, such as Palmer Drought Severity Index (PDSI) or precipitation minus evaporation (P-E), can provide conflicting answers about responses of drought to warming or overestimate aridification from warming (e.g., Trenberth et al., 2014; Swann et al., 2016). Furthermore, droughts are complex phenomena with various characteristics including intensity, duration, frequency, onset, demise, and areal extent. Here, implications of seasonal precipitation and temperature trends on seasonal droughts are examined as the issue of drought duration and severity have already been addressed in Ukkola, 2020.

2.2 Instrumental Data

The station-based Global Precipitation Climatology Centre (GPCC) version 2018 (Schneider et al., 2011), University of Delaware (UDEL) version 5.01 (Willmott and Matsuura, 2001), and National Oceanic and Atmospheric Administration (NOAA) Precipitation Reconstruction over Land (Chen et al., 2002; PRECL) are used to examine past rainfall variability and trends. When showing time series covering the 1979-2018 CE time period, the station-based data are supplemented with Climate Prediction Center Merged Analysis of Precipitation (CMAP) data set, which blends satellite and gauge-based data from 1979 CE to the present (Xie and Arkin, 1997). Past surface air temperature variability over land is also examined using Goddard Institute of Space Studies (GISS) surface temperature analysis (GISTEMP; Lenssen et al., 2019), Climate Research Unit (CRU) Air Temperature Anomalies version 4.2.0 (CRUTEMv4; Jones et al., 2014), and University of Delaware (UDEL) temperature version 5.01 (Willmott and Marsuura, 2001). Linear trends in each temperature and rainfall dataset are calculated over the 1950-2014 CE time period and the average of these trends are shown in Figure 1. Stippling in Figure 1 shows where all rainfall (GPCC, UDEL, PRECL) or temperature data (GISTEMP, CRUTEM4, UDEL) agree on the sign of trend over this time period. Varying the time period over which this trend is calculated (e.g., 1950-2010 or 1950-2017 CE) does not noticeably change these results.

In all instrumental time series (e.g., Figure 2), data are normalized to the mean and standard deviation (σ) of the 1950-2000 CE time period (hereafter 'baseline) using the mean and σ from all datasets that have coverage over this time period. The instrumental October-March 1950-2000 CE mean rainfall is 1230 mm (+/- 19 mm), and σ is 214mm (+/- 19mm). The October-March mean UDEL temperature over the baseline period is 22.4°C, and the average temperature σ across all three instrumental data sources is 0.34°C (+/-0.03°C). GISTEMP and CRUTEM4 provide temperatures as anomalies, so their mean 1950-2000 CE temperatures are not presented here. An anomalously 'hot' season is defined as a year when October-March mean temperatures are at least 2-σ above the baseline, and anomalously dry seasons are defined as October-March precipitation anomalies at least 1.5 σ below the baseline period. These thresholds are based on anomalously high temperatures and drought conditions experienced in this region during recent El Niño events (1982-1983, 1997-1998, 2015-2016; JM16; Figure 2).

2.3 Climate Model Data

Surface air temperature (tas) and precipitation (pr) from 25 models from Phase 6 of the Coupled Model Intercomparison Project (CMIP6) model simulations are used (Table S1). Precipitation and temperatures are examined using monthly data from the historical and Shared Socio-Economic Pathway (SSP) 3-7.0 experiments (Eyring et al., 2016; Riahi et al., 2017). The historical runs are driven by observed transient forcing (land use change, greenhouse gas, aerosol, ozone). The SSP simulations are high-end emissions scenarios from the Scenario Model Intercomparison Project (ScenarioMIP). These scenarios are concentration-driven experiments determined from hypothetical future socioeconomic pathways (Riahi et al., 2017). The SSP3-7.0 scenario reaches ~7.0 W/m^2 radiative forcing by 2100 in a 'regional rivalry' scenario (O'Neill et al., 2016). CMIP6 temperature and rainfall trends are compared to output from 32 CMIP5 historical and RCP8.5 simulations (CMIP5 models listed in Table S1). CMIP6 SSP3-7.0 results have been compared to CMIP6 SSP5-8.5 results, and the main conclusions are nearly identical (not shown).

CMIP6 model time series of eastern Amazonian rainfall and temperatures are shown as anomalies relative to the October-March mean and standard deviation (σ) 1950-2000 CE 'baseline'. In the CMIP6 historical simulations 1950-2000 CE, the mean October-March rainfall over eastern Amazonia is 926 mm (+/- 222 mm), and σ is 180mm (+/- 36mm). The October-March mean temperature is 22.4°C (+/-1.1°C), and σ is 0.60°C (+/-0.19°C). The CMIP6 models show a slightly wetter mean as compared to the CMIP5 simulations, which Yin et al., 2013 reported displayed a 'dry bias'; the CMIP5 (Table S1) mean 1950-2000CE October-March rainfall is 846 mm (+/-274 mm). However, the intent of this work is not to provide a detailed analysis of the causes for CMIP5 and CMIP6 differences in these models (e.g., Cook et al., 2020), but instead to discuss the implications of a drying a warming trend for the region.

2.4 Comparison with sea-surface temperature variability

Variability of sea-surface temperatures in the tropical Atlantic and Pacific is also compared to rainfall and temperature variability over land. Specifically, the El Niño Southern Oscillation (ENSO) index, calculated from the National Oceanic and Atmospheric Administration (NOAA) Extended Reconstructed Sea Surface Temperature version 5 (ERSSTv5) dataset (Huang et al., 2017), is compared with rainfall and temperature variability over land. The October-March Niño3.4 index (5ºS-5º N, 170º-120º W), and the Tropical North Atlantic index (6ºS-22º N, 80ºW-15º W) is compared with October-March rainfall and temperature over tropical South America over the 1950-2014 CE time period after removing the linear trend from each grid point over this time period. Maps of correlations show the average correlation between the ERSSTv5 Niño3.4 index and each precipitation dataset (GPCC, UDEL, PRECL) and temperature dataset (GISTEMP, CRUTEM4, UDEL), with stippling showing where all datasets agree on the sign of the correlation (Figure S2, Figure S3).

The CMIP6 historical and SSP3-7.0 rainfall and temperature over South America are also compared with the Niño3.4 index (5ºS-5º N, 170º-120º W) and Tropical North Atlantic index (6ºS-22º N, 80ºW-15º W). Specifically, the Niño3.4 index and TNA index are correlated in each CMIP6 model with rainfall and temperature over tropical South America separately over the 1950-2014 CE and 2015-2100 CE after removing the linear trend from each grid point over these time periods (Figure S2, Figure S3). Maps of correlations in Figures S2 and S3 show the average correlation among all CMIP6 simulations over the relevant time periods, with stippling showing where >90% models agree on sign of correlation.

3 Results

3.1 Trends in Amazonian Temperature and Rainfall

Instrumental data and CMIP6 simulations show similar warming trends 1950-2014 CE over northern Amazonia and much of southeastern Brazil (Figure 1). However, the CMIP6 multi-model mean shows a more widespread, homogeneous warming pattern than the instrumental data; this result is perhaps not surprising given that ensemble mean of climate model simulations tend to maximize forced variability (Knight et al., 2009). All CMIP6 models show a continued warming trend across the region (Figure 1) in the warming projections from the Shared Socio-Economic Pathway (SSP) 3-7.0 simulations).

Instrumental precipitation data show a drying trend over much of eastern Amazonia and northern tropical South America, and a positive rainfall trend in much of western Amazonia 1950-2014 CE (Figure 1). CMIP6 models show a drying trend over northern South America and much of southern Amazonia. However, under the SSP3-7.0 global warming scenario, >75% of models show that the drying trend expands over much of southwestern, eastern, and northern tropical South America. All but two months show future drying trends across much of Amazonia in CMIP6 projections (Figure S1). CMIP6 models show a different response to warming as compared to the CMIP5 21st century warming projections, which suggested that much of western Amazonia will become more wet while eastern Amazonia will receive less rainfall (Duffy et al., 2015; Cook et al., 2020).

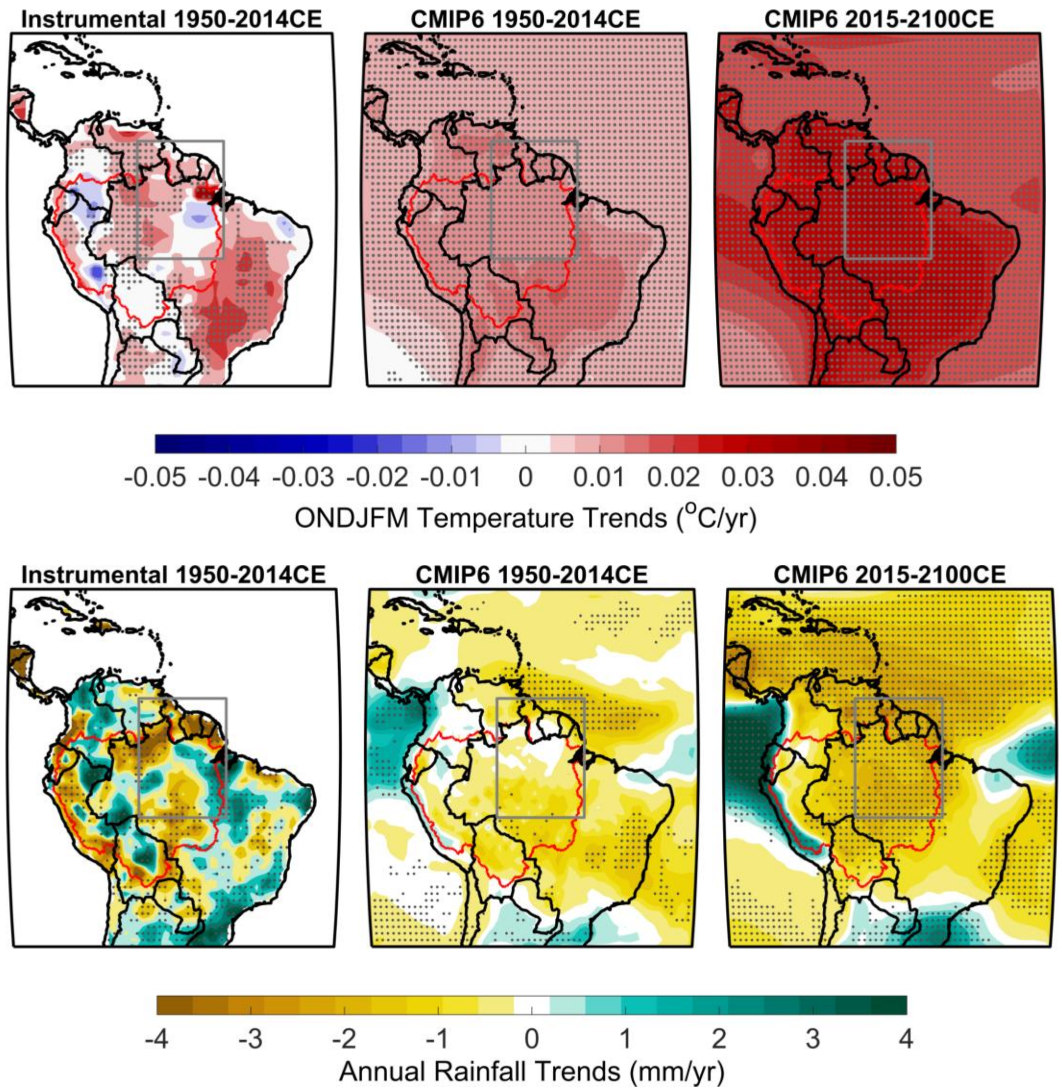

Figure 1. Temperature (top) and rainfall (bottom) trends in instrumental data 1950-2014 CE (left) climate model historical simulations 1950-2014 CE (middle), and in the SSP3-7.0 warming scenario 2015-2100 CE (right). Grey box outlines the Eastern Amazonian region used to make all time series shown in text (10ºS-8º N, 60ºW-50º W), red line outlines the Amazonian basin, and black lines show country borders. Precipitation and temperature trend maps show average trends across instrumental and model data (Methods). Stippling on maps shows where all instrumental data agree on sign of trend (left) or where more than 19 out of 25 model simulations (>75%) agree on the sign of the trend (middle, right).

3.2 Climate Change and the Shifting Risk of Amazonian Drought

Instrumental records of Amazonian rainfall and surface air temperatures extending to the early 20th century can be used to put recent 'enhanced droughts' in a longer-term context (JM16). Instrumental data show that recent October-March seasonal droughts associated with El Niño events have been 2-3 standard deviations (σ) warmer than the 1950-2000 CE baseline (Methods), with recent multi-year temperatures either at or near this 2 σ level (Figure 2). Recent low-rainfall seasons also appear more frequent than the mid 20th century, with multiple seasons since 1980

CE showing rainfall deficits at least 1.5-2 σ below the baseline. Although recent droughts appear abnormal, the time period ~1900-1940 CE also experienced several warm seasons nearly 2 σ above the 1950-2000 CE mean, and there were multiple dry events of lower magnitude during this time period (Figure 2). Given the lack of station data in the early 20th century (Figure 2), CMIP6 simulations are used to examine the shifting frequency of 2-σ seasonal temperature anomalies and -1.5 σ rainfall extremes.

CMIP6 historical simulations confirm the instrumental-based analysis, which shows that isolated warm years in Amazonia have occurred before the recent late 20th century and early 21st century warming. However, these models show that greenhouse gas driven warming is already increasing the frequency of these events (Figure 2). Specifically, by 2030 CE the average temperature in CMIP6 is 2 σ warmer than the baseline. Under unabated emissions, by mid-century, the coolest October-March seasons will be as warm as the isolated heat events of the recent past. By the end of the 21st century under unabated emissions, the average October-March season is 6-8 σ (3.6-4.8ºC) above the baseline, with the warmest seasons 12-20 σ (7.2-12ºC) above the baseline, and the coolest seasons at least as warm as the hottest droughts during El Niño events in the late 20th century and early 21st century.

Although all models show warming in the SSP3-7.0 scenario that exceeds internal variability, future rainfall trends do not exceed the envelope of 20th century variability in all CMIP6 simulations (Figure 2). However, a drying trend in almost all models increases the likelihood of seasonal droughts similar in magnitude to recent observed droughts. CMIP6 simulations show an average decrease in precipitation of ~0.5 σ relative to 1950-2000 CE by 2040 CE; around this time, these simulations project regular 1.5-2 σ seasonal rainfall deficits relative to the baseline every year. By the end of the 21st century if global warming is left unchecked, the average year in eastern Amazonia receives as much rainfall as a typical drought year in the 20th century, and particularly dry seasons approach 3-4 σ below the baseline.

The bottom panel in Figure 2 shows the shifting risk of these 'enhanced' droughts by decade. Starting in the 21st century, at least 10% of CMIP6 simulations cross the 2-σ heat threshold per decade, and by mid-century, all CMIP6 SSP3-7.0 simulations show that seasonal temperatures will cross this threshold at some point each decade. In addition to projecting large temperature increases, CMIP6 simulations show an increasing risk of rainfall deficits 1.5 σ below the baseline as well; in the coming decades (2020-2050 CE), between 0 and 20% of models cross this rainfall deficit threshold per decade. By mid-century, at least 10% of models show cross this drought threshold at least once per decade, and by 2080 CE, on average at least one in five models show 1.5 σ droughts at least once per decade.

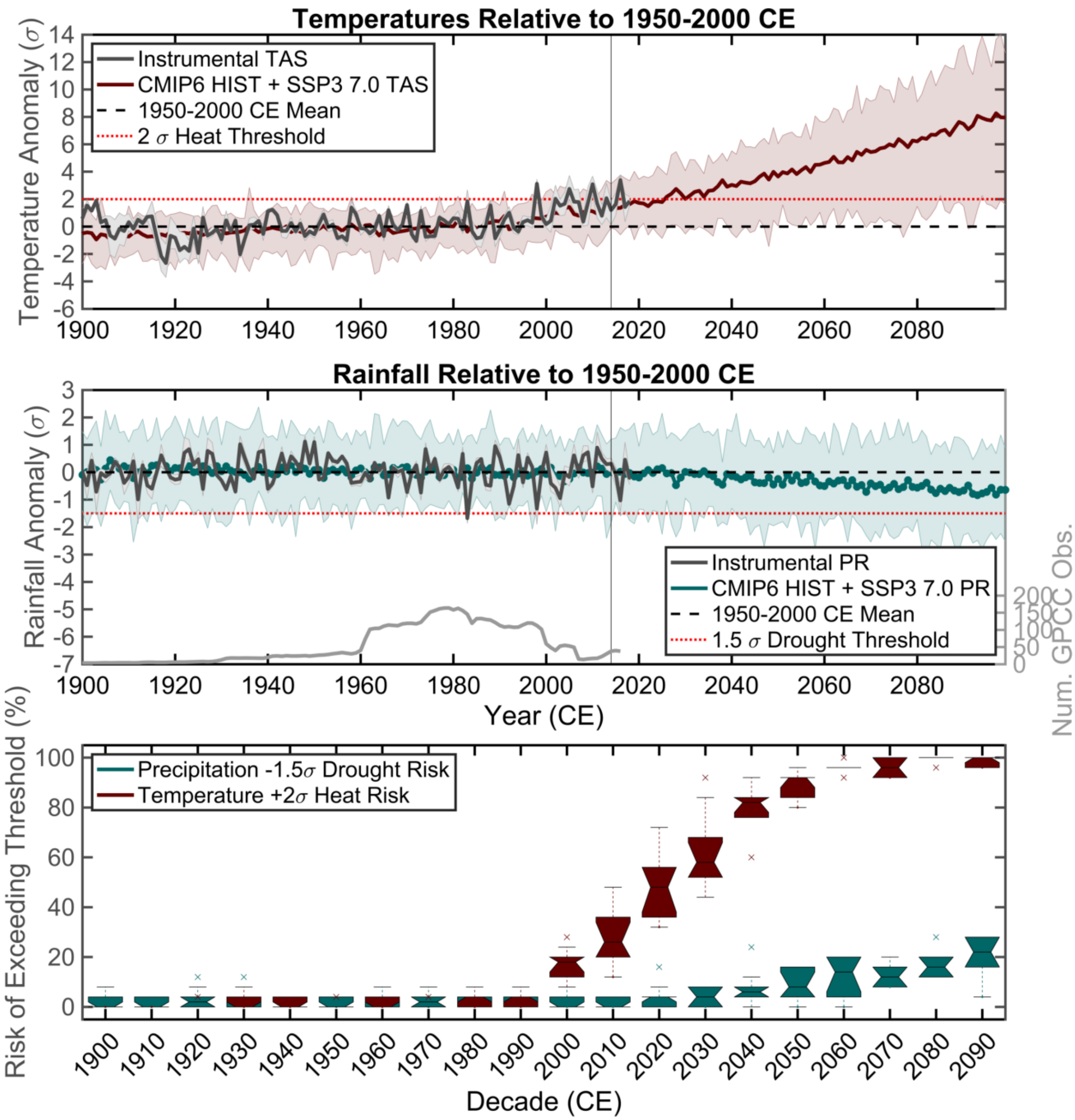

Figure 2. Top two panels show October-March temperature (top) and rainfall (middle) anomalies from the 1950-2000 CE time period in eastern Amazonia (10ºS-8º N, 60ºW-50º W) in instrumental data (grey) and CMIP6 historical and SSP3-7.0 simulations (blue). Thick light grey line on bottom of middle panel shows number of station observations in eastern Amazonia. Boxplots in bottom panel show the percent of years per decade that fall outside the baseline (1950-2000 CE) range of temperature and rainfall variability. Dashed black line shows the 1950-2000 CE mean, red dotted line shows the heat and drought thresholds, light grey lines show spread of instrumental data, and dark grey lines show mean of instrumental data. Vertical line shows the end of the historical simulations and the start of the SSP simulations. Dark blue lines show multi-model mean temperature and rainfall in the historical and SSP3-7.0 simulations, and

light blue lines show CMIP6 maxima and minima. See Methods for more information about instrumental data. Red boxplots show the spread in the percent of models per decade that exceed a 2-σ temperature threshold, and teal boxplots show the spread in the percent of models per decade that simulate droughts 1.5 σ below the baseline.

4 Discussion and Conclusions

Sea-surface temperature anomaly patterns in both the tropical Pacific and tropical Atlantic can help drive temperature and rainfall variability over northern South America (Yoon and Zeng, 2010; Kousky et al., 1984; Ropelewski and Halpert, 1987). Although seasonal droughts in southern Amazonia have been linked to the tropical North Atlantic (Yoon and Zeng, 2010), recent particularly warm droughts in central and eastern Amazonia have occurred during strong El Niño events (JM16). Future rainfall changes over Amazonia could be driven by a warming tropical Pacific (Barichivich et al., 2012). Indeed, CMIP6 simulations project a strengthening relationship between the tropical Pacific (Figure S2) and the tropical North Atlantic (Figure S3) in the 21st century over tropical South America.

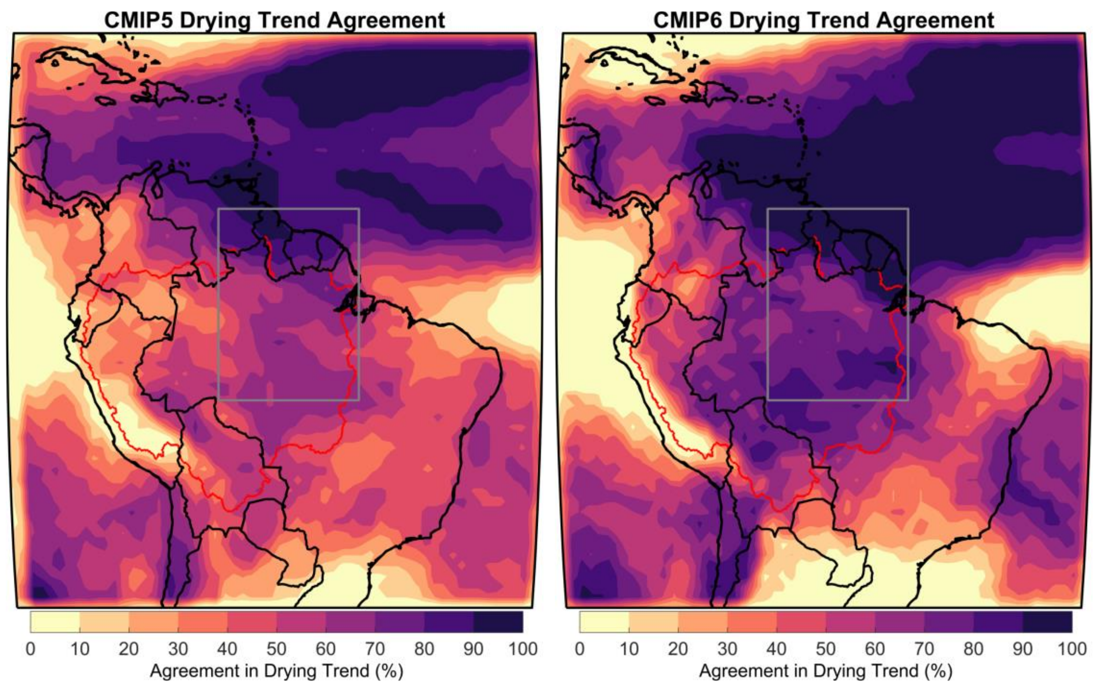

Figure 3. Agreement in sign of drying trend in CMIP5 RCP 8.5 (N=32) and CMIP6 SSP3-7.0 (N=25) 21st century warming simulations.

CMIP5 and CMIP6 models appear to show qualitatively similar relationships with the tropical Pacific and Atlantic, yet CMIP6 models more consistently simulate drying in Amazonia in the 21st century warming projections across the Amazonian basin in most seasons (Figure 1; Figure S1), whereas CMIP5 models show less agreement in future rainfall trends (Figure 3; Figure S4). Although a relationship between 21st century trends in the Niño3.4 index and trends in Amazonian rainfall is found (Figure 4), future global warming could independently cause increasing temperatures in the tropical Pacific while causing decreasing rainfall over Amazonia.

Therefore, west-east tropical Pacific temperature trend differences are compared to determine if the tropical Pacific becomes more 'El Niño like' or 'La Niña like' in the 21st century. CMIP6 models that simulate a more 'El Niño like' future tropical Pacific (stronger warming in the eastern Pacific relative to the western Pacific) tend to simulate more drying over Amazonia (Figure 4). Most CMIP6 models analyzed here indicate that the tropical Pacific will become more 'El Niño like' in the future; shifts in Walker circulation related to decreasing tropical Pacific SST gradient could explain much of the CMIP6 agreement in future drying trends over Amazonia. A similar comparison in 32 CMIP5 models indicates that the previous generation of models shows a similar relationship between the tropical Pacific SST and Amazonian rainfall. Specifically, several CMIP5 models simulate a more 'La Niña like' future tropical Pacific and minimal or no increasing rainfall trends over Amazonia (Figure 4).

Although there is better agreement in projected future rainfall trends in CMIP6 models in many regions (e.g., Cook et al., 2020; Ukkola et al., 2020), these results should be interpreted with caution for several reasons. Most CMIP6 models show future drying in Amazonia, but the local details of this drying pattern can vary from model to model (Figure S5). Future work should examine the causes of increased CMIP6 agreement in rainfall trends in the region, as well as why certain models, such as INM-CM4-8 and INM-CM5-0, appear to show increasing future rainfall in many parts of tropical South America (Figure S5). Additionally, treating individual model simulations from a Modeling Intercomparison Project as independent can be problematic because multiple, similar models from the same modeling centers are often included (Table S1), and models from different centers often share similar components (e.g., Knutti et al., 2013). Also, climate models from different modeling centers can agree on the sign of a projected precipitation trend, but this agreement could be based on the same systematic bias that appears across models (e.g., Tierney et al., 2015).

Future changes in the tropical Pacific are uncertain, and recent work has shown that CMIP5 models show considerable tropical Pacific biases, so future trends in tropical Pacific gradients and their potential impacts on tropical rainfall could be incorrect (e.g., Seager et al., 2019). Furthermore, climate model simulations may underestimate dry-season length (Marengo et al., 2017) as well as the risk of multi-year droughts in Amazonia (Parsons et al., 2017), so the potential for multi-year dry periods superimposed on background warming and potential drying trends in CMIP6 projections should be considered (Marengo et al., 2018). Recent work has also shown that the December-May season may in fact have experienced increasing rainfall trends 1979-2015 CE in northwestern Amazonia (Fu et al., 2013). CMIP6 historical simulations do simulate positive rainfall trends in northeastern Amazonia (1950-2014 CE) in several of these months (Figure S1), although these trends are apparent in the October-March seasonal average as well (Figure 1). Additionally, the work presented here has not explored the length of the dry or onset of rainy season (Marengo et al., 2011; 2017; Fu et al., 2013; Ukkola et al., 2020), or how temperature and rainfall changes can impact other drought metrics in CMIP6 projections such as soil moisture content (e.g., Cook et al., 2020).

Nonetheless, if CMIP6 simulations of future drying in the America Tropics are accurate, these results are especially relevant given recent developments in Amazonia related to land management, drought, and fires. The Amazonian forest appears to be particularly vulnerable to forest fire and land clearing during drought (Nepstad et al., 2008; Le Page et al., 2017), particularly for forest edges where drying, fire intensity, and grass invasion are greatest (Balch et al., 2015). Given that rainfall deficits on their own can increase fire risk and forest dieback, this region appears susceptible to self-amplified forest loss and a possible deforestation tipping point (Brando et al., 2014; Zemp et al., 2017; Boers et al., 2017). Without significant local land management efforts combined with global efforts to curtail carbon emissions, this region appears increasing vulnerable to warming, drought, fire, and land use conversion (Marengo et al., 2018). Forest dieback driven by these combined stressors would, in turn, have major implications for regional carbon sequestration and biodiversity and the global climate system.

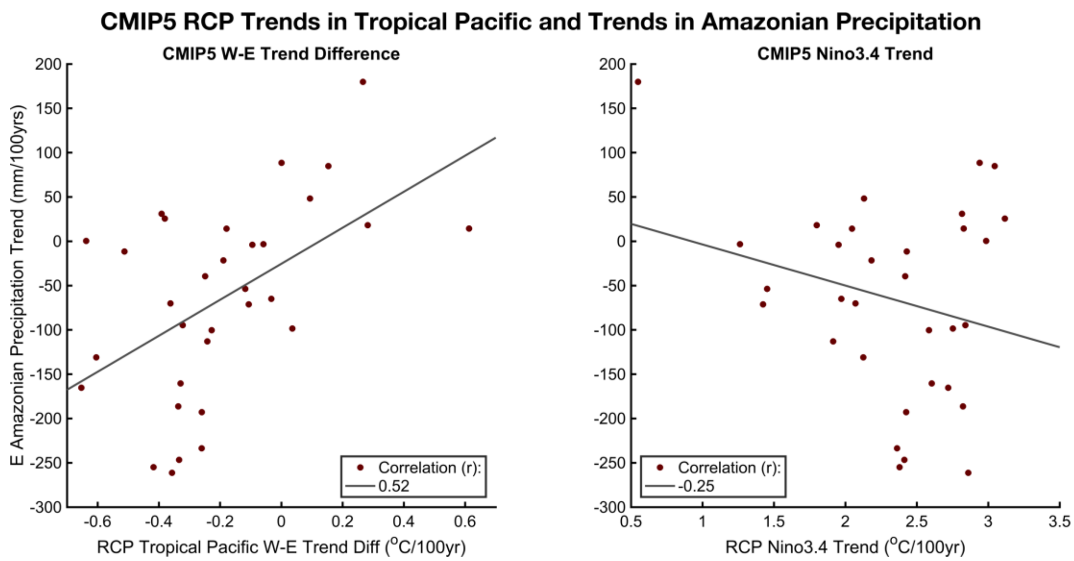

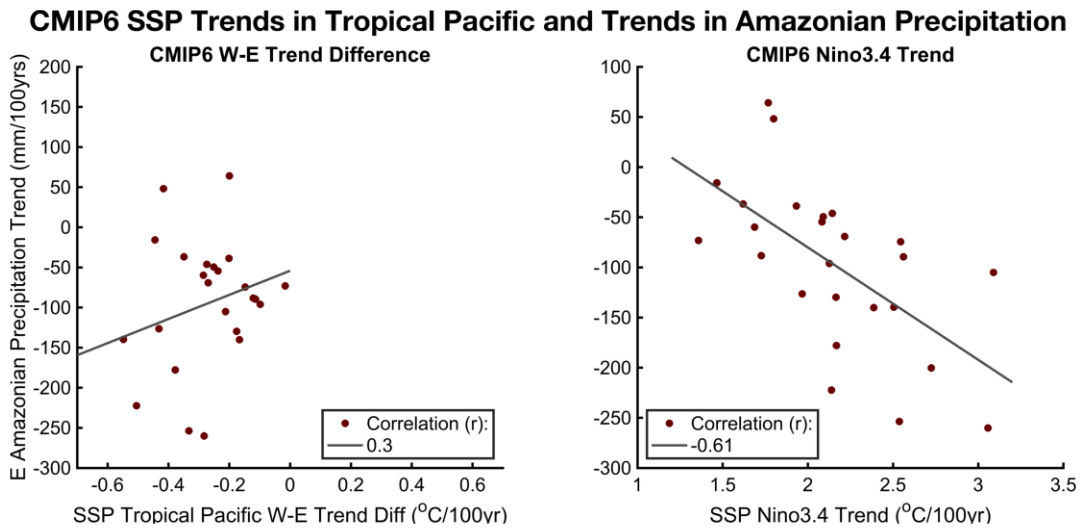

Figure 4. Relationship between October-March temperature trends in the tropical Pacific and eastern Amazonian rainfall in CMIP5 RCP8.5 (2006-2099 CE) and CMIP6 SSP3-7.0 simulations (2015-2099 CE). Difference in western tropical Pacific and eastern tropical Pacific temperature trends (Methods) and eastern Amazonian rainfall trends (left) and Niño3.4 temperature trends and eastern Amazonian rainfall trends (right).

Acknowledgments

The author thanks the Washington Research Foundation for their funding support through the WRF Postdoctoral Fellowship. The author also thanks T Ault, A Swann, D Frierson, G Hakim, E Steig, and J Overpeck for input and support. Observation-based gridded temperature and precipitation data provided by the NOAA/OAR/ESRL PSD, Boulder, Colorado, USA, from their Web site at https://www.esrl.noaa.gov/psd/. Coupled Model Intercomparison Project Phase 6 (CMIP6) data were downloaded from the World Climate Research Programme (WCRP) Earth System Grid Federation (ESGF) website: https://esgf-node.llnl.gov/search/cmip6/.

References

Aragão, L. E., L. O. Anderson, M. G. Fonseca, T. M. Rosan, L. B. Vedovato, F. H. Wagner, C. V. Silva, C. H. S. Junior, E. Arai, and A. P. Aguiar (2018), 21st Century drought-related fires counteract the decline of Amazon deforestation carbon emissions, *Nature communications, 9*, 536.

Boers, N., N. Marwan, H. M. Barbosa, and J. Kurths (2017), A deforestation-induced tipping point for the South American monsoon system, *Sci. Rep., 7*, 41489.

Brando, P. M. et al. (2014), Abrupt increases in Amazonian tree mortality due to drought–fire interactions, *Proceedings of the National Academy of Sciences, 111*, 6347-6352.

Bush, M. B., A. Correa-Metrio, C. H. McMichael, S. Sully, C. R. Shadik, B. G. Valencia, T. Guilderson, M. Steinitz-Kannan, and J. T. Overpeck (2016), A 6900-year history of landscape modification by humans in lowland Amazonia, *Quat. Sci. Rev., 141*, 52-64.

Chen, M., P. Xie, J. E. Janowiak, and P. A. Arkin (2002), Global land precipitation: A 50-yr monthly analysis based on gauge observations, *J. Hydrometeorol., 3*, 249-266.

Cook, B. I., J. S. Mankin, K. Marvel, A. P. Williams, J. E. Smerdon, and K. J. Anchukaitis , Twenty-first Century Drought Projections in the CMIP6 Forcing Scenarios*, Earth's Future*, e2019EF001461.

Dai, A. (2013), Increasing drought under global warming in observations and models*, Nature Climate Change, 3*, 52-58.

Davidson, E. A. et al. (2012), The Amazon basin in transition*, Nature, 481*, 321.

Diffenbaugh, N. S. and F. Giorgi (2012), Climate change hotspots in the CMIP5 global climate model ensemble*, Clim. Change, 114*, 813-822.

Duffy, P. B., P. Brando, G. P. Asner, and C. B. Field (2015), Projections of future meteorological drought and wet periods in the Amazon*, Proceedings of the National Academy of Sciences, 112*, 13172-13177.

Frankcombe, L. M., M. H. England, J. B. Kajtar, M. E. Mann, and B. A. Steinman (2018), On the choice of ensemble mean for estimating the forced signal in the presence of internal variability*, J. Clim., 31*, 5681-5693.

Huang, B., P. W. Thorne, V. F. Banzon, T. Boyer, G. Chepurin, J. H. Lawrimore, M. J. Menne, T. M. Smith, R. S. Vose, and H. Zhang (2017), Extended reconstructed sea surface temperature, version 5 (ERSSTv5): upgrades, validations, and intercomparisons*, J. Clim., 30*, 8179-8205.

Jimenez-Munoz, J. C., C. Mattar, J. Barichivich, A. Santamaria-Artigas, K. Takahashi, Y. Malhi, J. A. Sobrino, and G. van der Schrier (2016), Record-breaking warming and extreme drought in the Amazon rainforest during the course of El Nino 2015-2016*, Sci Rep, 6*, 33130.

Jones, P. D., D. H. Lister, T. J. Osborn, C. Harpham, M. Salmon, and C. P. Morice (2012), Hemispheric and large- scale land- surface air temperature variations: An extensive revision and an update to 2010*, Journal of Geophysical Research: Atmospheres, 117*.

Knight, J. R. (2009), The Atlantic Multidecadal Oscillation Inferred from the Forced Climate Response in Coupled General Circulation Models*, J. Climate, 22*, 1610-1625.

Knutti, R., Masson, D., & Gettelman, A. (2013). Climate model genealogy: Generation CMIP5 and how we got there. *Geophys. Res. Lett*., 40(6), 1194-1199.

Kousky, V. E., M. T. Kagano, and I. F. Cavalcanti (1984), A review of the Southern Oscillation: oceanic- atmospheric circulation changes and related rainfall anomalies*, Tellus A, 36*, 490-504.

Le Page, Y., D. Morton, C. Hartin, B. Bond-Lamberty, J. M. C. Pereira, G. Hurtt, and G. Asrar (2017), Synergy between land use and climate change increases future fire risk in Amazon forests*, Earth System Dynamics (Online), 8*.

Lehner, F., S. Coats, T. F. Stocker, A. G. Pendergrass, B. M. Sanderson, C. C. Raible, and J. E. Smerdon (2017), Projected drought risk in 1.5 C and 2 C warmer climates*, Geophys. Res. Lett., 44*, 7419-7428.

Lenssen, N. J., G. A. Schmidt, J. E. Hansen, M. J. Menne, A. Persin, R. Ruedy, and D. Zyss (2019), Improvements in the GISTEMP Uncertainty Model*, Journal of Geophysical Research (Atmospheres), 124*, 6307-6326.

Lenton, T. M., H. Held, E. Kriegler, J. W. Hall, W. Lucht, S. Rahmstorf, and H. J. Schellnhuber (2008), Tipping elements in the Earth's climate system*, Proc. Natl. Acad. Sci. U. S. A., 105*, 1786-1793.

Lewis, S. L., P. M. Brando, O. L. Phillips, van der Heijden, Geertje M. F., and D. Nepstad (2011), The 2010 Amazon Drought*, Science, 331*, 554.

Malhi, Y., Aragao, Luiz E. O. C., D. Galbraith, C. Huntingford, R. Fisher, P. Zelazowski, S. Sitch, C. McSweeney, and P. Meir (2009), Exploring the likelihood and mechanism of a climate-change-induced dieback of the Amazon rainforest*, Proc. Natl. Acad. Sci. U. S. A., 106*, 20610-20615.

Malhi, Y., J. T. Roberts, R. A. Betts, T. J. Killeen, W. Li, and C. A. Nobre (2008), Climate change, deforestation, and the fate of the Amazon*, Science, 319*, 169-172.

Marengo, J. A., J. Tomasella, L. M. Alves, W. R. Soares, and D. A. Rodriguez (2011), The drought of 2010 in the context of historical droughts in the Amazon region*, Geophys. Res. Lett., 38*, L12703.

Marengo, J. A., G. F. Fisch, L. M. Alves, N. V. Sousa, R. Fu, and Y. Zhuang (2017), Meteorological context of the onset and end of the rainy season in Central Amazonia during the 2014-15 Go-Amazon Experiment*, Atmos.Chem.Phys.Discuss.*

Marengo, J. A., C. A. Souza, K. Thonicke, C. Burton, K. Halladay, R. A. Betts, and W. R. Soares (2018), Changes in climate and land use over the Amazon Region: current and future variability and trends*, Frontiers in Earth Science, 6*, 228.

Mittermeier, R. A., N. Myers, J. B. Thomsen, G. A. Da Fonseca, and S. Olivieri (1998), Biodiversity hotspots and major tropical wilderness areas: approaches to setting conservation priorities*, Conserv. Biol., 12*, 516-520.

NEPSTAD, D. C., C. R. DECARVALHO, E. A. DAVIDSON, P. H. JIPP, P. A. LEFEBVRE, G. H. NEGREIROS, E. D. DASILVA, T. A. STONE, S. E. TRUMBORE, and S. VIEIRA (1994), The Role of Deep Roots in the Hydrological and Carbon Cycles of Amazonian Forests and Pastures*, Nature, 372*, 666-669.

Nepstad, D. C., C. M. Stickler, B. S. Filho, and F. Merry (2008), Interactions among Amazon land use, forests and climate: prospects for a near-term forest tipping point*, Philosophical Transactions of the Royal Society B: Biological Sciences, 363*, 1737-1746.

O'Neill, B. C., C. Tebaldi, D. P. v. Vuuren, V. Eyring, P. Friedlingstein, G. Hurtt, R. Knutti, E. Kriegler, J. Lamarque, and J. Lowe (2016), The scenario model intercomparison project (ScenarioMIP) for CMIP6*, Geoscientific Model Development, 9*, 3461-3482.

Osborn, T. J., C. J. Wallace, I. C. Harris, and T. M. Melvin (2016), Pattern scaling using ClimGen: monthly-resolution future climate scenarios including changes in the variability of precipitation*, Clim. Change, 134*, 353-369.

Osborn, T. J., C. J. Wallace, J. A. Lowe, and D. Bernie (2018), Performance of Pattern-Scaled Climate Projections under High-End Warming. Part I: Surface Air Temperature over Land*, J. Clim., 31*, 5667-5680.

Parsons, L. A., S. LeRoy, J. T. Overpeck, M. Bush, G. M. Cárdenes- Sandí, and S. Saleska , The Threat of Multiyear Drought in Western Amazonia*, Water Resour. Res.*

Phillips, O. L. et al. (2009), Drought Sensitivity of the Amazon Rainforest*, Science, 323*, 1344-1347.

Riahi, K., D. P. Van Vuuren, E. Kriegler, J. Edmonds, B. C. O'neill, S. Fujimori, N. Bauer, K. Calvin, R. Dellink, and O. Fricko (2017), The shared socioeconomic pathways and their energy, land use, and greenhouse gas emissions implications: an overview*, Global Environ. Change, 42*, 153-168.

Ropelewski, C. F. and M. S. Halpert (1987), Global and regional scale precipitation patterns associated with the El Niño/Southern Oscillation*, Mon. Weather Rev., 115*, 1606-1626.

Saatchi, S., S. Asefi-Najafabady, Y. Malhi, Aragao, Luiz E. O. C., L. O. Anderson, R. B. Myneni, and R. Nemani (2013), Persistent effects of a severe drought on Amazonian forest canopy*, Proc. Natl. Acad. Sci. U. S. A., 110*, 565-570.

Saeed, F., I. Bethke, E. Fischer, S. Legutke, H. Shiogama, D. A. Stone, and C. Schleussner (2018), Robust changes in tropical rainy season length at 1.5 C and 2 C*, Environmental Research Letters, 13*, 064024.

Satyamurty, P., A. A. de Castro, J. Tota, S. G. da, and A. O. Manzi (2010), Rainfall trends in the Brazilian Amazon Basin in the past eight decades*, Theoretical and Applied Climatology, 99*, 139-148.

Schneider, U., A. Becker, P. Finger, A. Meyer-Christoffer, B. Rudolf, and M. Ziese (2011), Monthly Land-Surface Precipitation from Rain-Gauges Built on GTS-Based and Historic Data*, Global Precip.Climatol.Cent.(GPCC), Deutscher Wetterdienst, doi, 10*.

Seager, R., M. Cane, N. Henderson, D. Lee, R. Abernathey, and H. Zhang (2019), Strengthening tropical Pacific zonal sea surface temperature gradient consistent with rising greenhouse gases*, Nature Climate Change, 9*, 517.

Soares, W. R., J. A. Marengo, and C. A. Nobre (2019), Assessment of warming projections and probabilities for brazil, in *Climate Change Risks in Brazil*Anonymous , pp. 7-30, Springer.

Swann, A. L., F. M. Hoffman, C. D. Koven, and J. T. Randerson (2016), Plant responses to increasing CO2 reduce estimates of climate impacts on drought severity*, Proceedings of the National Academy of Sciences, 113*(36), 10019-10024.

Taylor, K. E., R. J. Stouffer, and G. A. Meehl (2012), An Overview of Cmip5 and the Experiment Design*, Bull. Am. Meteorol. Soc., 93*, 485-498.

Tian, H., J. M. Melillo, D. W. Kicklighter, A. D. McGuire, J. V. Helfrich, B. Moore, and C. J. VoÈroÈsmarty (1998), Effect of interannual climate variability on carbon storage in Amazonian ecosystems*, Nature, 396*, 664-667.

Tierney, J. E., C. C. Ummenhofer, and P. B. deMenocal (2015), Past and future rainfall in the Horn of Africa*, Science advances, 1*(9), e1500682.

Trenberth, K. E., A. Dai, G. Van Der Schrier, P. D. Jones, J. Barichivich, K. R. Briffa, and J. Sheffield (2014), Global warming and changes in drought*, Nature Climate Change, 4*(1), 17-22.

Ukkola, A. M., M. G. De Kauwe, M. L. Roderick, G. Abramowitz, and A. J. Pitman (2020), Robust future changes in meteorological drought in CMIP6 projections despite uncertainty in precipitation.

Wang, X., X. Li, J. Zhu, and C. A. Tanajura (2018), The strengthening of Amazonian precipitation during the wet season driven by tropical sea surface temperature forcing*, Environmental Research Letters, 13*, 094015.

Willmott, C. J. and K. Matsuura (2001), Terrestrial air temperature and precipitation: Monthly and annual time series (1950–1999) Version 1.02*, Center for Climatic Research, University of Delaware, Newark*.

Xie, P. and P. A. Arkin (1997), Global precipitation: A 17-year monthly analysis based on gauge observations, satellite estimates, and numerical model outputs*, Bull. Am. Meteorol. Soc., 78*, 2539-2558.

Yeh, S., Y. Ham, and J. Lee (2012), Changes in the tropical Pacific SST trend from CMIP3 to CMIP5 and its implication of ENSO*, J. Clim., 25*, 7764-7771.

Yin, L., R. Fu, E. Shevliakova, and R. E. Dickinson (2013), How well can CMIP5 simulate precipitation and its controlling processes over tropical South America?, *Clim. Dyn., 41*, 3127-3143.

Yoon, J. and N. Zeng (2010), An Atlantic influence on Amazon rainfall, *Clim. Dyn., 34*, 249-264.

Zemp, D. C., C. Schleussner, H. M. Barbosa, M. Hirota, V. Montade, G. Sampaio, A. Staal, L. Wang-Erlandsson, and A. Rammig (2017), Self-amplified Amazon forest loss due to vegetation-atmosphere feedbacks, *Nature Communications, 8*, 14681.